



Proceeding Paper

# Flood Vulnerability Mapping Using MaxEnt Machine Learning and Analytical Hierarchy Process (AHP) of Kamrup Metropolitan District, Assam †

Akshayasimha Channarayapatna Harshasimha and Chandra Mohan Bhatt \*

Indian Institute of Remote Sensing, Dehradun 248001, India; akshaysimhachhp@gmail.com

\* Correspondence: cmbhatt@iirs.gov.in

† Presented at the 7th International Electronic Conference on Water Sciences, 15–30 March 2023; Available online: <https://ecws-7.sciforum.net>.

**Abstract:** Addressing a natural hazard's complexity is essential in preventing human fatalities and conserving natural ecosystems as natural hazards are varied and unbalanced in both time and place. Therefore, the main objective of this study is to present a flood vulnerability hazard map and its evaluation for hazard management and land use planning. The flood inventory map is generated for different flood locations using multiple official reports. To generate the vulnerability maps, a total of nine geo-environmental parameters are chosen as predictors from Maximum Entropy (MaxEnt) machine learning and Analytical Hierarchy Process (AHP). Accuracy assessment of the outputs from MaxEnt is performed using the area under the curve. Similarly, for AHP outputs, the accuracy is tested using the generated inventory map and the AUC. It is observed that topographical wetness index, elevation, and slope are significant for the assessment of flooded areas. Finally, flood hazard maps are generated and a comparative analysis is performed for both methods. According to the study's findings, The AUC of the flood map generated by MaxEnt is 0.83, whereas the AUC of the flood map generated by AHP is 0.76, which means that the flood map generated by MaxEnt is better. From this study, it can be concluded that hazard maps could be a useful tool for local authorities to identify places that are vulnerable to hazards on a large scale.

**Keywords:** vulnerability mapping; Maximum Entropy (MaxEnt); Analytical Hierarchy Process (AHP); area under the curve (AUC)



**Citation:** Harshasimha, A.C.; Bhatt, C.M. Flood Vulnerability Mapping Using MaxEnt Machine Learning and Analytical Hierarchy Process (AHP) of Kamrup Metropolitan District, Assam. *Environ. Sci. Proc.* **2023**, *25*, 73. <https://doi.org/10.3390/ECWS-7-14301>

Academic Editor: Athanasios Loukas

Published: 3 April 2023



**Copyright:** © 2023 by the authors. Licensee MDPI, Basel, Switzerland. This article is an open access article distributed under the terms and conditions of the Creative Commons Attribution (CC BY) license (<https://creativecommons.org/licenses/by/4.0/>).

## 1. Introduction

Around the world, natural catastrophes pose a major threat to property and human lives. Although it is impossible to prevent natural hazards, their negative impact can be reduced by creating effective planning strategies and mitigation techniques. Significant morphological changes in landforms brought on by active tectonics or climatic changes may affect human activity and management. Events such as gully erosion, landslides, and floods are physical phenomena that are active in geological times but uneven in time and space [1–4].

According to (NDMA, 2008), a flood is extra water due to a river being incapable of transferring a large amount of water from the upstream area within its banks after significant rainfall. Floods occur more frequently and are more damaging to local social, economic, and environmental aspects than all other natural catastrophes that occur on a global scale. High intensity precipitation in the watershed, changes in river cross sections caused by sedimentation, sudden dam failure, release of high flow from dams, etc., are just a few causes of floods.

Depending on a variety of criteria that includes velocity, geography, and source, floods can be broadly classified into four categories: fluvial (river) floods, ground water floods, pluvial floods, and surge (coastal) floods. Assam, which is in the monsoon climatic region,

has been having an average yearly rainfall from 1600 mm to 4300 mm, causing flooding throughout the region (Assam State Disaster Management, n.d.). Overflowing tributaries of the Brahmaputra River also contribute to the volume of flood water in the valley.

Furthermore, this state has unique hydrological, climatic, and unstable geological conditions that intensify the source of numerous geomorphic and geological dangers in the region. Considering all these conditions, the use of remote sensing techniques proves to be a viable solution.

## 2. Study Area

The Kamrup Metropolitan district, which is located in the state of Assam in the north-eastern part of India, covers an area of 1528 km<sup>2</sup>. The study area stretches from 26.07° N latitude to 91.63° E longitude in the lower basin of Brahmaputra, which is prone to rapid flooding nearly every year (Figure 1).

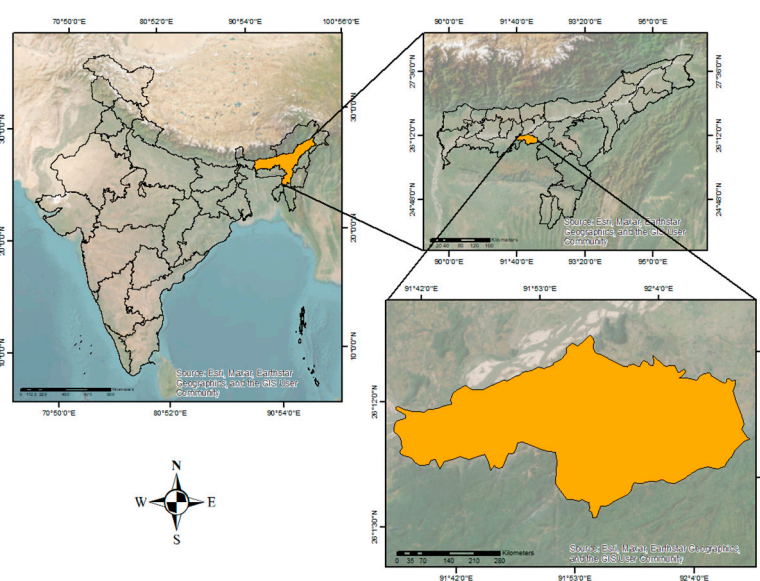


**Figure 1.** Research study area of the Kamrup Metropolitan district, Assam, India.

In 2021, the districts of Assam had an average annual temperature of 24 °C and an annual rainfall of over 2200 mm. The Kamrup Metropolitan district has major cities and is Assam's administrative center.

## 3. Materials and Methods

Figure 2 illustrates the methodology that was approached with AHP modeling and MaxEnt modeling.

### 3.1. Flood Inventory Mapping

A key step for susceptibility mapping is the preparation of an inventory of hazard landforms. The flood inventory for the Kamrup Metropolitan district (Assam, India) is compiled from national and regional documents from various organizations such as Assam State Disaster Management Authority and the North-Eastern Space Applications Centre. About 53 flood areas are listed on the inventory map for floods. For training samples, a random partition approach is used. In the present study, 70% of each hazard is considered for model construction (training) and the remaining 30% of each hazard is used for validation.

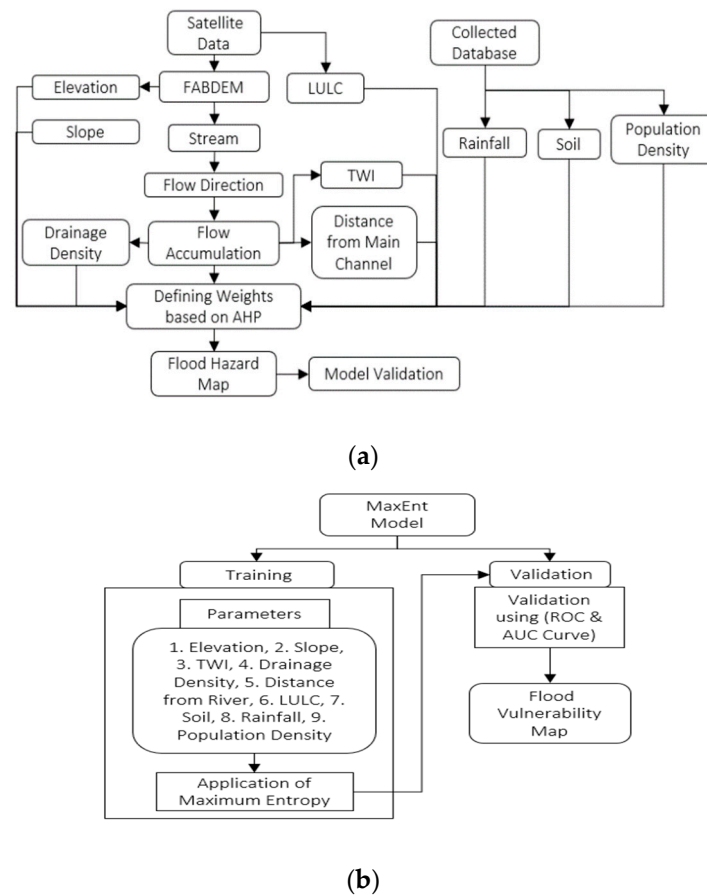


**Figure 2.** (a) AHP flowchart; (b) MaxEnt flowchart.

### 3.2. Flood Conditioning Factors

It is essential to determine the effective factors of different natural hazards and human-made fatalities to perform flood maps [5]. A good understanding of the main hazard-related factors is needed to recognize the susceptible areas.

For this aim, the conditioning factors for the hazard were selected [6–10]. In this study, ArcGIS 10.3 (ESRI, USA) is used to perform the analysis of AHP and to produce and display the data layers. All the factors were processed into a raster grid of 30 × 30 m grid cells. Entire conditioning factors were primarily continuous, and some of them were classified within different categories based on expert knowledge and a literature review [11–14].

#### 3.2.1. Elevation

Elevation is a parameter of great significance for delineating flood hazards and mapping flood zones. During the monsoon, the downstream area generates ideal flood conditions due to sedimentation and surge in river flow. Understanding elevation variation is critical for river basin generation and the propagation of flood waters. In this study, FABDEM (Forest and Building removed Copernicus DEM) data with a spatial resolution of 30 m is used.

#### 3.2.2. Slope

The steepness and length of a region’s topography greatly influence its discharge and flooding. The rapid velocity of precipitation runoff is caused by steep or high slopes. Low or flat slopes, on the other hand, are prone to waterlogging, which can lead to high infiltration. The slope map was created using FABDEM (DEM) data.

The geo-environmental parameters used in this study are presented Figure 3 below.

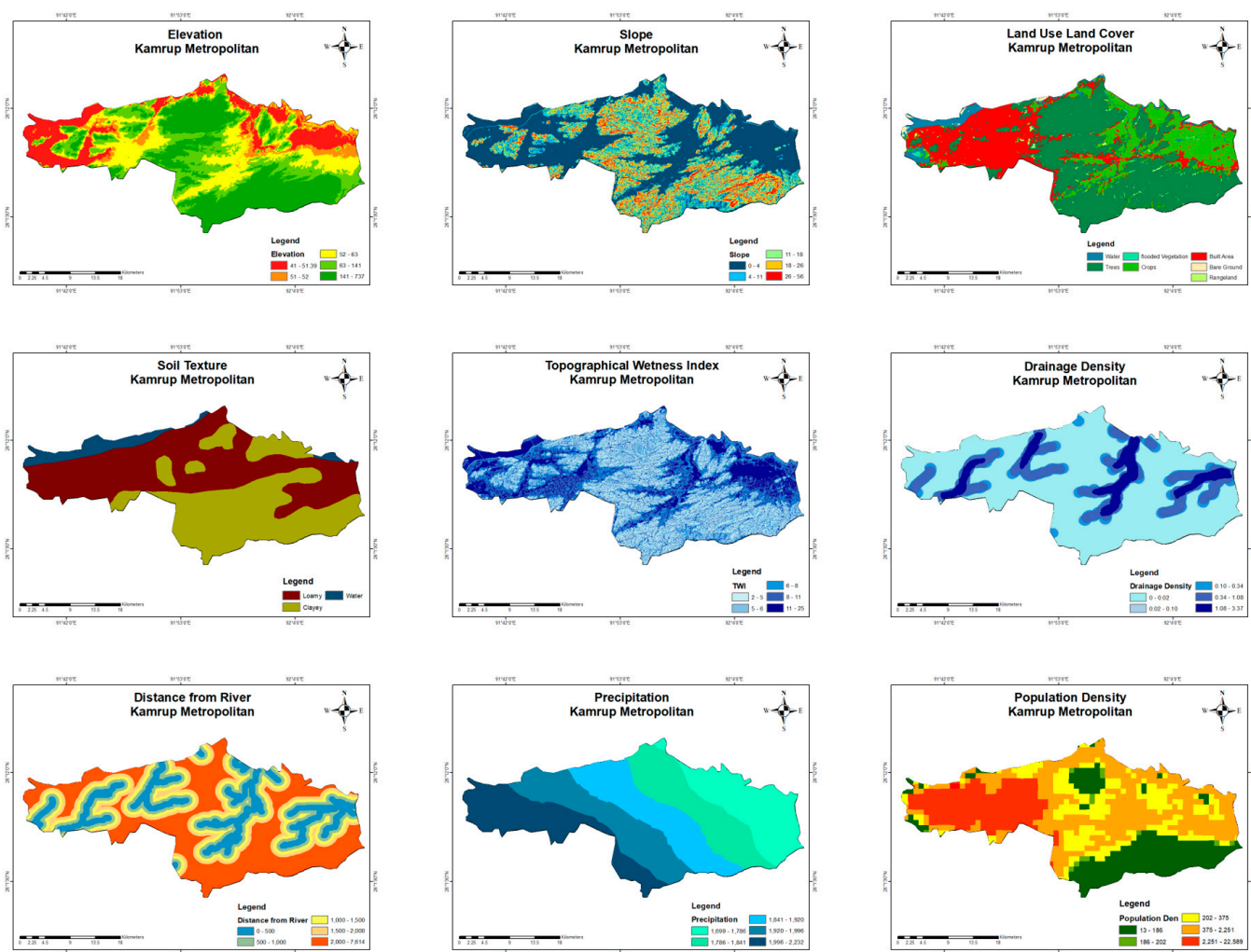


Figure 3. Nine geo-environmental conditioning factors.

### 3.2.3. Land Use Land Cover

Land use/land cover plays a significant role in the operation of hydrological and geomorphological processes by directly or indirectly influencing processes such as evapotranspiration, infiltration, runoff generation, and sediment dynamics. The land use/land cover product with a 10 m spatial resolution is obtained from Sentinel-2 using the Google Earth Engine (GEE) platform.

### 3.2.4. Soil Texture

Soil texture is generally recognized not only as a weighty controlling factor in the mechanism of infiltration and runoff generation but also as being effective for hazard occurrence. This layer was acquired from the NBSSLUP. The soil texture in the study area comprises loam and clay.

### 3.2.5. Topographic Wetness Index (TWI)

Moore and Grayson [15] and Grabs et al. [16] mention that TWI (Topographic wetness index) represents how the tendency of gravitational forces and the spatial distribution of wetness conditions move water down slope. This layer was generated using DEM. TWI is also important in the regulation of surface runoff since the wetter an area is, the greater its runoff will be.

### 3.2.6. Distance from River Channel

The distance from the river was estimated in ArcGIS using the Euclidean Distance tool, which displays the distance from the river basin region to the natural drainage. In this context, natural drainage refers to all streams and rivers in the study region, which was categorized into five classes: 500 m, 1000 m, 1500 m, and 2000 m.

### 3.2.7. Drainage Density

The primary influencing factor that contributes to the occurrence of numerous risks is drainage density. A higher surface runoff ratio results from a higher drainage density. To convert the drainage network pattern to a measurable quantity, the drainage density was determined using an extension of “line density” in ArcGIS 10.3 software.

### 3.2.8. Rainfall

Rainfall is a key aspect in this study as floods most commonly occur during monsoon season, hence the term “rain-induced floods”. The rainfall map of the study area is generated using the Inverse Distance Weighted approach (IDW) from Global Precipitation Measurement datasets. The map is generated considering the annual total rainfall of year 2021 as 2021 was a flood year.

### 3.2.9. Population Density

One of the critical elements to consider while conducting flood vulnerability research is population density. This component is important for analyzing the social loss and damage suffered by communities in flood-vulnerable areas as a result of floods. The population density map for the study area is obtained from Google Earth Engine databases of population density gridded data with  $\approx 1$  km of spatial resolution.

## 4. Results

### 4.1. Maximum Entropy (MaxEnt)

The MaxEnt software uses the Maximum Entropy model to calculate hazard estimates (version 3.4.4). The MaxEnt model is usually used to estimate species distribution based on the most significant environmental conditions. From a decision-theoretic perspective, we also interpret the maximum entropy estimation as a reliable Bayes estimation. The model relies on a machine learning reaction that generates hypotheses based on skewed data. The result from the model is obtained in ASCII format. The conditioning factors are translated from raster into ASCII format, as required by the software. The most crucial phase in the modeling process is validation. The AUC has been used to assess the built-in hazard model’s prediction accuracy, as shown in Figure 4.

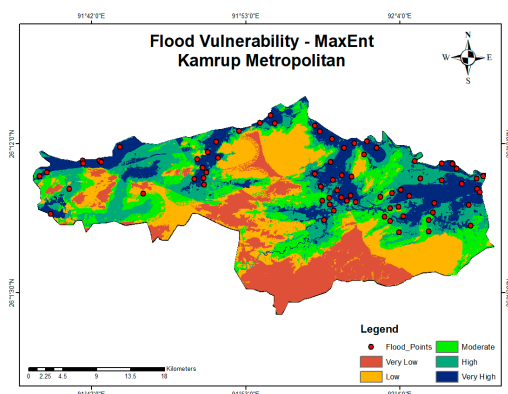


Figure 4. MaxEnt flood mapping.

#### 4.2. Analytical Hierarchy Process (AHP)

Table 1 shows the weights assigned to the nine geo-environmental parameters used to generate the flood hazard map. To obtain the spatial distribution of flood hazards, the parameters evaluated were mapped and normalized into five classes based on a rating scale of 1 to 5, with 1 being the least vulnerable area and 5 being the most vulnerable area, as shown in Figure 5.

Table 1. AHP weights.

Factor	Weight
Slope	0.22
Distance from River channel in meter	0.17
Land use land cover	0.05
Soil Texture	0.10
Elevation	0.07
Rainfall in mm	0.04
Population Density	0.02
TWI	0.21
Drainage Density	0.12

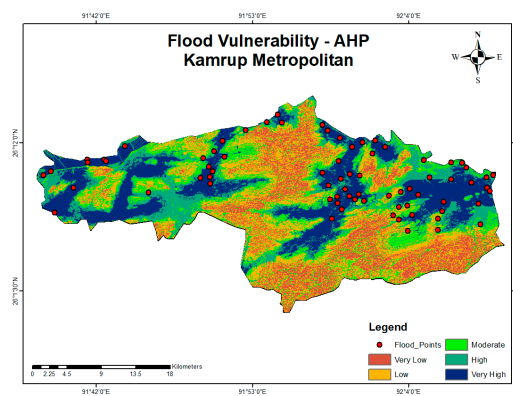


Figure 5. AHP flood Mapping.

#### 4.3. Comparative Analysis of sensitivity and Response Curves

The relative influence of each predictor variable on the outcomes of the predicted maps using the jackknife test was examined using a sensitivity analysis from the AUC. Concerning validating with respect to flood inventory points, we observe that the 0.83 AUC of the MaxEnt model slightly outperformed the 0.763 AUC of the AHP model, as shown in Figures 6 and 7, respectively.

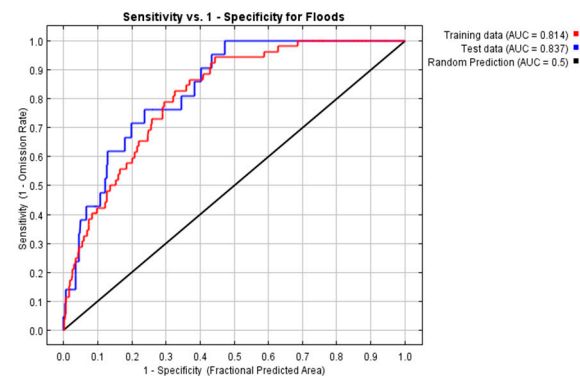
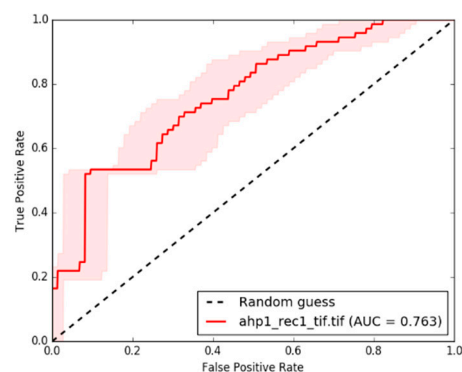


Figure 6. AUC for MaxEnt.



**Figure 7.** AUC for AHP.

#### 4.4. Spatial Extent of Vulnerability

Flood vulnerability maps generated from the outputs of MaxEnt and AHP show that the areas encircling the river, the surfaces with slopes from 0 degrees to 11 degrees, and the land in the elevation range from 41 m to 52 m showed vulnerability to floods. Subsequently, we observe that the flood map generated by MaxEnt and AHP showed a reasonable resemblance with the historical flood maps of ISRO's Bhuvan.

From the results, we also observe that out of the 1528 km<sup>2</sup> total area of the district, about 650 km<sup>2</sup> was found to be highly vulnerable to floods; moreover, major locations such as Guwahati, Dispur, and Sonapur Gaon in the Kamrup Metropolitan district showed a higher vulnerability to flooding.

### 5. Conclusions

In this study, flood vulnerability maps are generated for a major district of Assam by utilizing the AHP approach and MaxEnt machine learning. Given its ability to handle huge datasets, a multi-criteria analysis using AHP and MaxEnt identified and proven to be beneficial for flood risk assessment.

Slope, drainage density, TWI, and elevation were the primary flood-causing geo-environmental parameters in the studied area. The AHP method and MaxEnt technique employed in this study are effective and enable the possibility of further research into flood vulnerabilities in various sections of the state or country. The AUC graphs are employed as a validation method in this work, which demonstrates an additional possibility of research validation and applicability in geospatial vulnerability assessment owing to extreme events.

**Author Contributions:** The initial idea for the work came from A.C.H. with assistance from mentor C.M.B., who is also a corresponding author on this publication. The records, compilation, and choice of the final design of the work were done by A.C.H. All authors contributed to this paper and shared ideas. All authors have read and agreed to the published version of the manuscript.

**Funding:** This research received no external funding.

**Institutional Review Board Statement:** Not applicable.

**Informed Consent Statement:** Not applicable.

**Data Availability Statement:** Not applicable.

**Conflicts of Interest:** The authors declare no conflict of interest.

### References

1. Achour, Y.; Pourghasemi, H.R. How do machine learning techniques help in increasing accuracy of landslide susceptibility maps. *Geosci. Front.* **2020**, *11*, 871–883. [[CrossRef](#)]
2. Arnaud, P.; Bouvier, C.; Cisneros, L.; Dominguez, R. Influence of rainfall spatial variability on food prediction. *J. Hydrol.* **2002**, *260*, 216–230. [[CrossRef](#)]
3. Castillo, C.; Gómez, J.A. A century of gully erosion research: Urgency, complexity and study approaches. *Earth-Sci. Rev.* **2016**, *160*, 300–319. [[CrossRef](#)]

4. Kelarestaghi, A.; Ahmadi, H. Landslide susceptibility analysis with a bivariate approach and GIS in Northern Iran. *Arab. J. Geosci.* **2009**, *2*, 95–101. [[CrossRef](#)]
5. Kia, M.B.; Pirasteh, S.; Pradhan, B.; Mahmud, A.R.; Sulaiman WN, A.; Moradi, A. An artificial neural network model for food simulation using GIS: Johor River Basin Malaysia. *Environ. Earth Sci.* **2012**, *67*, 251–264. [[CrossRef](#)]
6. Kornejady, A.; Ownegh, M.; Rahmati, O.; Bahremand, A. Landslide susceptibility assessment using three bivariate models considering the new topo-hydrological factor: HAND. *Geocarto Int.* **2018**, *33*, 1155–1185. [[CrossRef](#)]
7. Pourghasemi, H.; Moradi, H.; Aghda, S.F.; Gokceoglu, C.; Pradhan, B. GIS-based landslide susceptibility mapping with probabilistic likelihood ratio and spatial multi-criteria evaluation models (North of Tehran, Iran). *Arab. J. Geosci.* **2014**, *7*, 1857–1878. [[CrossRef](#)]
8. Rahmati, O.; Pourghasemi, H.R.; Melesse, A.M. Application of GIS-based data driven random forest and maximum entropy models for groundwater potential mapping: A case study at Mehran Region Iran. *CATENA* **2016**, *137*, 360–372. [[CrossRef](#)]
9. Tehrany, M.S.; Pradhan, B.; Jebur, M.N. Flood susceptibility mapping using a novel ensemble weights-of-evidence and support vector machine models in GIS. *J. Hydrol.* **2014**, *512*, 332–343. [[CrossRef](#)]
10. Conoscenti, C.; Rotigliano, E.; Cama, M.; Caraballo-Arias, N.A.; Lombardo, L.; Agnesi, V. Exploring the effect of absence selection on landslide susceptibility models: A case study in Sicily Italy. *Geomorphology* **2016**, *261*, 222–235. [[CrossRef](#)]
11. Das, H.; Sonmez, H.; Gokceoglu, C.; Nefeslioglu, H. Influence of seismic acceleration on landslide susceptibility maps: A case study from NE Turkey (the Kelkit Valley). *Landslides* **2013**, *10*, 433–454. [[CrossRef](#)]
12. Jiménez-Perálvarez, J.; Irigaray, C.; El Hamdouni, R.; Chacón, J. Landslide- susceptibility mapping in a semi-arid mountain environment: An example from the southern slopes of Sierra Nevada (Granada, Spain). *Bull. Eng. Geol. Environ.* **2011**, *70*, 265–277. [[CrossRef](#)]
13. Saponaro, A.; Pilz, M.; Wieland, M.; Bindi, D.; Moldobekov, B.; Parolai, S. Landslide susceptibility analysis in data-scarce regions: The case of Kyrgyzstan. *Bull. Eng. Geol. Environ.* **2015**, *74*, 1117–1136. [[CrossRef](#)]
14. Jaafari, A.; Najaf, A.; Pourghasemi, H.; Rezaeian, J.; Sattarian, A. GIS-based frequency ratio and index of entropy models for landslide susceptibility assessment in the Caspian forest, northern Iran. *Int. J. Environ. Sci. Technol.* **2014**, *11*, 909–926. [[CrossRef](#)]
15. Moore, I.D.; Grayson, R.B. Terrain-based catchment partitioning and runoff prediction using vector elevation data. *Water Resour. Res.* **1991**, *27*, 1177–1191. [[CrossRef](#)]
16. Grabs, T.; Seibert, J.; Bishop, K.; Laudon, H. Modeling spatial patterns of saturated areas: A comparison of the topographic wetness index and a dynamic distributed model. *J. Hydrol.* **2009**, *373*, 15–23. [[CrossRef](#)]

**Disclaimer/Publisher’s Note:** The statements, opinions and data contained in all publications are solely those of the individual author(s) and contributor(s) and not of MDPI and/or the editor(s). MDPI and/or the editor(s) disclaim responsibility for any injury to people or property resulting from any ideas, methods, instructions or products referred to in the content.